Time-Dependent Ginzburg—Landau Simulations of the Critical Current in Superconducting Films and Junctions in Magnetic Fields

A. I. Blair & D. P. Hampshire

Durham University, Centre for Materials Physics, Superconductivity Group, Department of Physics, DH1 3LE, UK

E-mail: a.i.blair@durham.ac.uk

4MP3-01

EPSRC

FUSION CDT

Introduction

We are trying to:

- Model and understand the critical current density of polycrystalline superconductors in high magnetic fields to optimise the design of magnets for fusion devices.
- Investigate the magnetic field dependence of the critical current across a single junction using simulations based on time-dependent Ginzburg—Landau (TDGL) theory.
- Exploit the significant increases in computational power in recent decades to model the electromagnetic properties of high field superconducting materials more accurately.

Time-Dependent Ginzburg—Landau Simulations

Time-Dependent Ginzburg—Landau Equations

The normalised TDGL equations can be written [1, 2]

$$\eta(\partial_t + \imath\Phi)\psi = [(\nabla - \imath\boldsymbol{A})^2 + \epsilon(\boldsymbol{r}) - |\psi|^2]\,\psi \quad \text{in } \Omega,$$

$$\kappa^2(\nabla\times\nabla\times\boldsymbol{A}) = \mathrm{Im}[\psi^*(\nabla - \imath\boldsymbol{A})\psi] + (-\nabla\Phi - \partial_t\boldsymbol{A}) \quad \text{in } \Omega,$$

with required boundary conditions

$$(\nabla\times\boldsymbol{A} - \boldsymbol{B})\times\hat{\boldsymbol{n}} = \boldsymbol{0} \quad \text{on } \partial\Omega,$$
$$(\nabla - \imath\boldsymbol{A})\psi\cdot\hat{\boldsymbol{n}} = -\gamma\psi \quad \text{on } \partial\Omega.$$

We have solved these equations in 2D using the finite-difference Crank-Nicolson algorithm employed by Winiecki and Adams [3] based on the link variable approach taken by Gropp et al. [4].

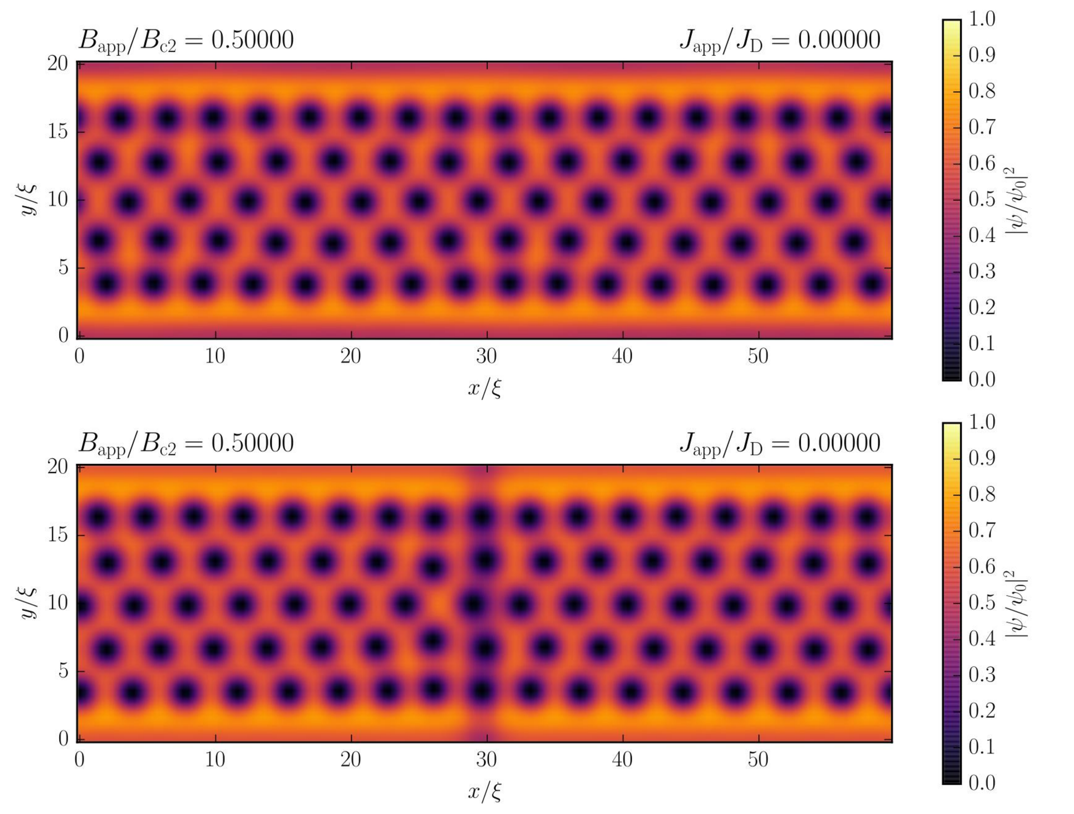

Fig. 1: Superelectron density $|\psi|^2$ normalised to the superelectron density in bulk Meissner state $|\psi_0|^2$, as a function of position in a superconducting film with $\eta = 1$ and $\kappa = 10$ at an applied external magnetic field $B_{app} = 0.5\,B_{c2}$. The system is periodic in the x-direction and insulating boundary conditions are applied in the y direction. A hexagonal vortex lattice is observed in the bulk of the superconducting film. Top: film; bottom: film containing central $2\,\xi$ wide junction with $\epsilon = 0.8$.

Computational System

In general we parameterise the superconductor using $\kappa = 10$, $\eta = 1$, $\epsilon = 1$ and a width $w = 20\,\xi$. Simple junctions are modelled as a central region $2\,\xi$ wide with $\epsilon = \epsilon_{\mathrm{Junc}}$.

Periodic boundary conditions are imposed in the x-direction. Second-order boundary conditions are imposed at the boundaries in the y-direction that describe either insulating ($\gamma = 0$) or highly metallic ($\gamma = \infty$) surfaces [5].

We have neglected effects from current flow outside the superconducting material, so the external magnetic fields and applied transport currents along the x direction are implemented using [6]

$$B\left(y = \frac{w}{2} \pm \frac{w}{2}\right) = B_{\mathrm{app}} \pm \frac{w}{2}\mu_0 J_{\mathrm{app}}.$$

Thin Films

E(*J*) Characteristics for Thin Films

Three regimes are observable in simulated $E(J)$ characteristics for wide thin films:

- (Almost) dissipationless current flow occurs at low transport currents.
- E-field oscillations are observed in the flux-flow regime from vortex motion.
- There is a distinct E-field transition to the normal state that becomes less abrupt at high fields.

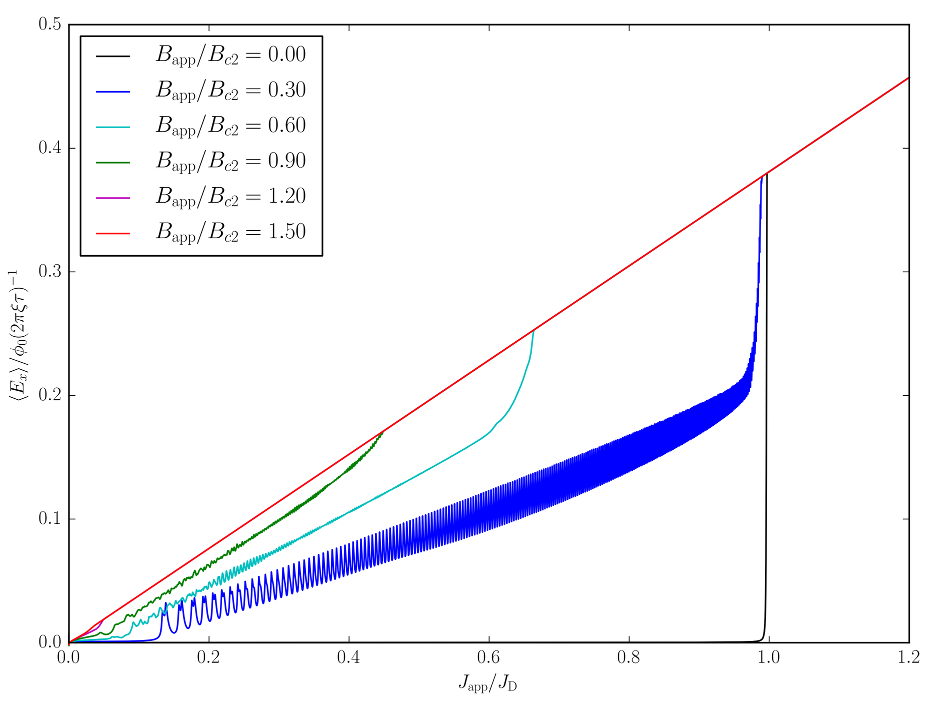

Fig. 2: Average electric field $\langle E_x\rangle$ against applied current density J_{app} for a superconducting film with $\eta = 1$ and $\kappa = 10$, subject to various external magnetic fields. After equilibration at a fixed external magnetic field, the external current density J_{ext} was slowly swept up above the depairing current J_{D} at a rate of $3\times10^{-6}J_{\mathrm{D}}\tau^{-1}$. Three regimes can clearly be seen in the data.

Width-dependent $J_c(B)$ Characteristics

Ekin's offset criterion was used to determine J_{c} [7] from $E(J)$ characteristics.

- Films that are wide relative to the coherence length exhibit a (distorted) Fraunhöfer-like dependence at low fields, close to their respective initial vortex penetration field.
- J_{c} decreases to zero above B_{c2} (for metallic surfaces) or B_{c3} (insulating surfaces) for wide films.
- For thin films subject to metallic boundary conditions, J_{c} drops to zero at all magnetic fields as film thickness decreases.
- For thin films subject to insulating boundary conditions, J_{c} only drops to zero close to the parallel critical field $B_{\mathrm{c}||} = \frac{2\sqrt{3}B_{\mathrm{c2}}\xi}{w}$, which can be very large [8].

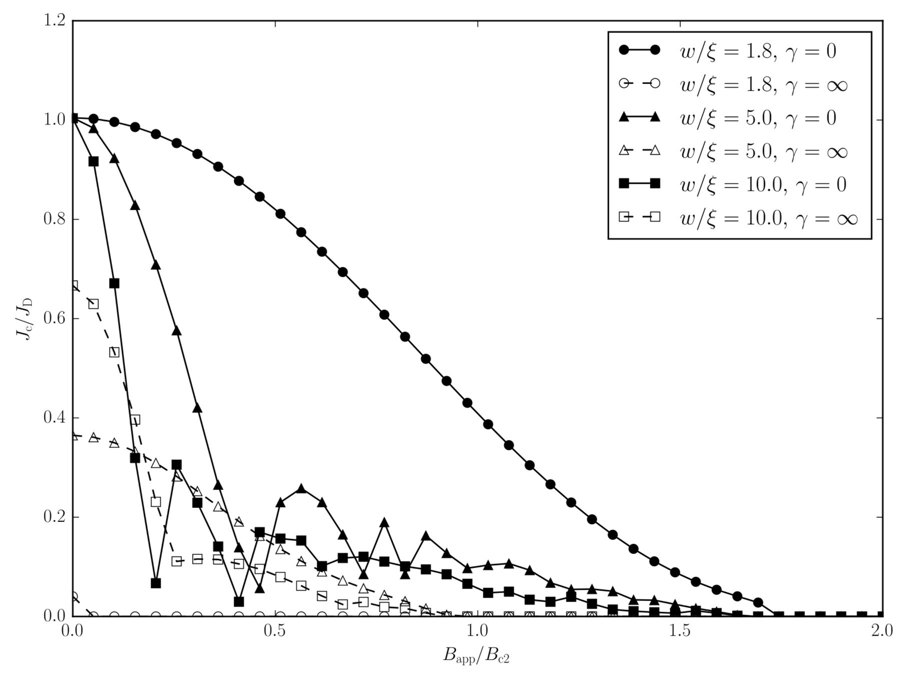

Fig. 3: Critical current density J_{c} against the external applied magnetic field B_{app} for a superconducting film with $\eta = 1$ and $\kappa = 10$ at various film widths. The critical current density was determined using Ekin's offset method from $E(J)$ characteristics computed at each magnetic field, using a critical electric field $E_{\mathrm{c}} = 0.01\,\phi_0/2\pi\xi\tau$.

Thin Films Containing Junctions

E(*J*) Characteristics for Thin Films with Junctions

The $E(J)$ characteristics for thin films are modified when junction regions are added:

- Electric field oscillations associated with vortex-antivortex annihilation along the junction were observed at large currents.
- The transition into the normal state is broadened by a supercurrent contribution at high transport currents.

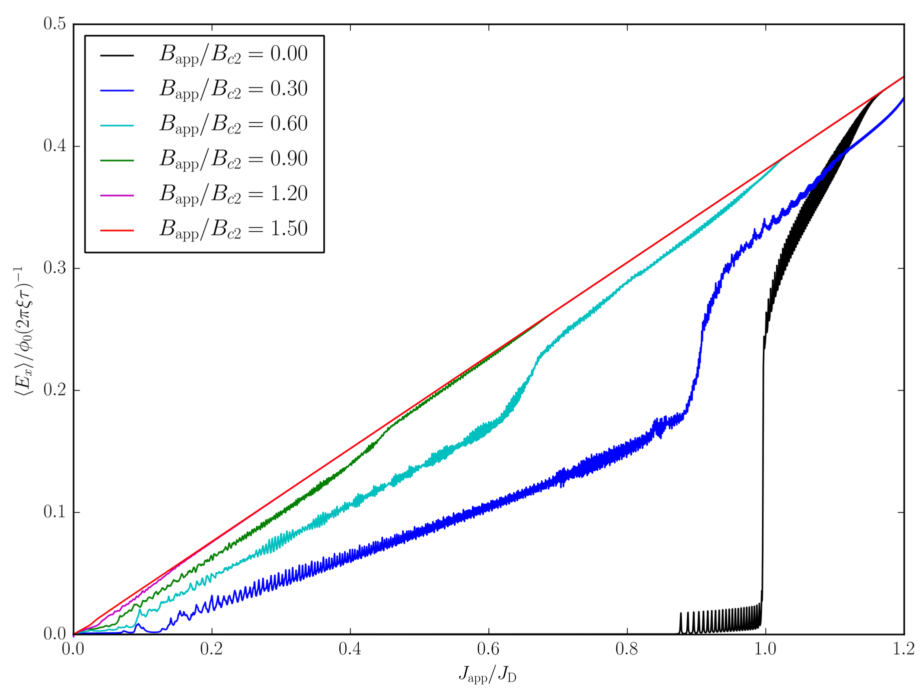

Fig. 4: Average electric field $\langle E_x\rangle$ against external applied current J_{app} for a superconducting film with $\eta = 1$ and $\kappa = 10$, containing a central $2\,\xi$ wide junction with $\epsilon = 0.8$ subject to various external magnetic fields.

Effect of Junction Properties on *E*(*J*) Characteristics in Zero Field

As ϵ_{Junc} decreases, T_{c} decreases in the junction and the $E(J)$ characteristics differ more strongly from the films:

- In the low E-field regime, J_{c} decreases as ϵ_{Junc} decreases.
- In the high E-field regime, the transition to the normal state broadens as ϵ_{Junc} decreases, and a higher transport current density is required to drive the whole system into the normal state.

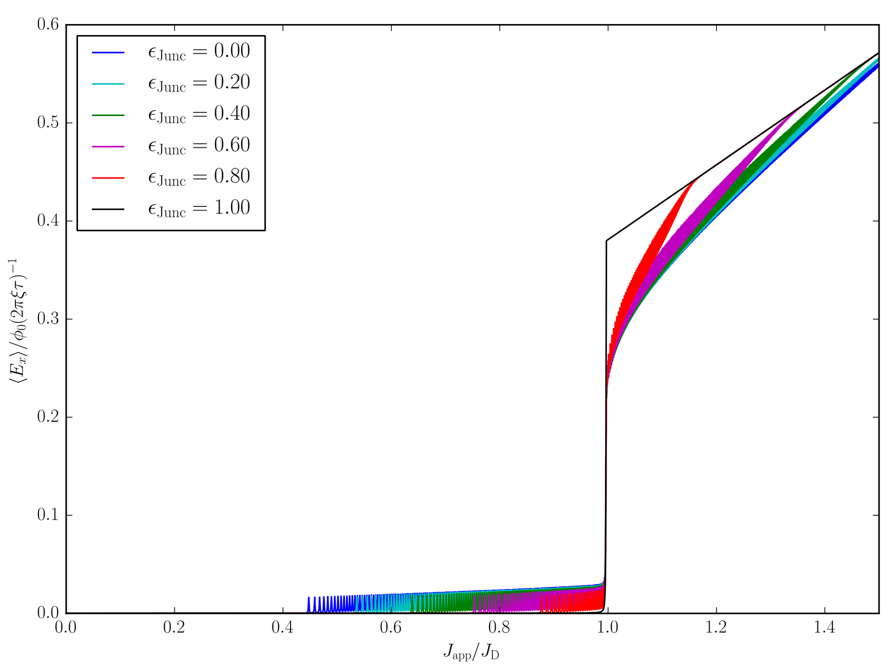

Fig. 5: Average electric field $\langle E_x\rangle$ against external applied current J_{app} for a superconducting film with $\eta = 1$ and $\kappa = 10$, containing a central $2\,\xi$ wide junction with $\epsilon = \epsilon_{\mathrm{Junc}}$, for various ϵ_{Junc} at zero field.

Conclusions

- $J_{\mathrm{c}} = J_{\mathrm{D}}$ for thin films with insulating boundary conditions in zero applied field .
- The critical current in thin films with insulating surfaces is limited by the parallel critical field $B_{\mathrm{c}||} = 2\sqrt{3}B_{\mathrm{c2}}\xi/w$, consistent with Tinkham's analytic results. The critical current of thin films in contact with highly metallic surfaces, in contrast, decreases to zero as the film width decreases.
- In zero applied field J_{c} decreases in thin films when junctions are added.
- The transition into the normal state at high currents is broadened for films containing junctions.

Future Work

We next plan to:

- Generate J_{c} data for thin films containing junctions in high magnetic fields.
- Investigate the effect of including junctions with η and κ values different to the surrounding superconductor.
- Extend the simulations to 3D and investigate $E(J)$ and $J_{\mathrm{c}}(B)$ behaviour in polycrystalline systems.

References and Acknowledgements

1. Gor'kov, L.P. and G.M. Eliashberg, *Generalization of the Ginzburg-Landau equations for non-stationary problems in the case of alloys with paramagnetic impurities.* Soviet Physics JETP, 1968. **27**(2): p. 328-334.
2. Sadovskyy, I.A., et al., *Stable large-scale solver for Ginzburg–Landau equations for superconductors.* Journal of Computational Physics, 2015. **294**: p. 639-654.
3. Winiecki, T. and C.S. Adams, *A Fast Semi-Implicit Finite Difference Method for the TDGL Equations.* Journal of Computational Physics, 2002. **179**: p. 127-139.
4. Gropp, W.D., et al., *Numerical simulation of vortex dynamics in Type-II superconductors.* Journal of Computational Physics, 1996. **123**: p. 254-266.
5. De Gennes, P.G., *Superconductivity of Metals and Alloys*. 1999, Boulder, Colorado: Perseus Books Group.
6. Machida, M. and H. Kaburaki, *Direct simulation of the time-dependant Ginzburg-Landau equation for Type-II superconducting thin film: Vortex dynamics and V-I characteristics.* Physical Review Letters, 1993. **71**(19): p. 3206-3209.
7. Ekin, J.W., *Experimental Techniques for Low-Temperature Measurements*. 2007, Oxford University Press: New York. p. 573.
8. Tinkham, M., *Introduction to Superconductivity*. 2nd ed. 1996, Singapore: McGraw-Hill Book Co.

This work is funded by EPSRC grant EP/L01663X/1 for the Fusion Doctoral Training Network. This work has been carried out within the framework of the EUROfusion Consortium and has received funding from the Euratom research and training programme 2014-2018 under grant agreement No 633053. Data are available at: http://dx.doi.org/10.15128/r15d86p0202 and associated materials are on the Durham Research Online website: http://dro.dur.ac.uk/. We also thank P. Branch for useful discussions.